SURFACE PRESSURE PREDICTION BY MEANS OF STATISTICS AND THE VORTICITY PRINCIPLE

by

VESNA JURCEC

B.S., The University of Zagreb
(1952)

SUBMITTED IN PARTIAL FULFILLMENT OF THE
REQUIREMENTS FOR THE DEGREE OF
MASTER OF SCIENCE

at the

MASSACHUSETTS INSTITUTE OF TECHNOLOGY
(1960)

Signature redacted

Signature of Author . . . . . .

Department of Meteorology, August 22, 1960

Signature redacted

Certified by . .
Thesis Supervisor

Signature redacted

. . . . . .
Chairman, Departmental Committee on Graduate Students

SURFACE PRESSURE PREDICTION BY MEANS OF STATISTICS AND THE VORTICITY PRINCIPLE

by

VESNA JURCEC

SUBMITTED IN PARTIAL FULFILLMENT OF THE REQUIREMENTS FOR THE DEGREE OF MASTER OF SCIENCE

ABSTRACT

The object of this thesis was to explore the possibility of improving the statistical surface pressure prediction through the use of 500-millibar vorticity data.

The test was made with surface pressure and 500-millibar height and vorticity data for January and February 1951. The statistical prediction was based on the pressure data from 24 and 36 hours previously. A reduction of error of .63 was obtained by using the pressure 24 hours previously, whereas the reduction of error was .70 when using the data of both 24 and 36 hours previously.

The combination of the statistical method with the methods containing the upper level vorticity field did not show any improvement over the statistical method alone. However, the results indicated that a slight improvement could be made by using the 500-millibar height change in conjunction with the statistical method.

Upon the investigation of the causes of the largest error, on February 1, when cyclogenesis occurred, it was suggested, at least in such a case, that it might be beneficial to include the temperature or thickness field in the statistical prediction.

Thesis Supervisor: Edward N. Lorenz
Title: Associate Professor of Meteorology

TABLE OF CONTENTS

SURFACE PRESSURE PREDICTION BY MEANS OF STATISTICS AND THE VORTICITY PRINCIPLE

I. INTRODUCTION

Statistical weather prediction methods may be used to determine the future state of the atmosphere as a function of its past state. These methods are not new, but now application of them is much more feasible because of the development of high-speed computers.

In statistical forecasting one requires a vast amount of information. For example, in the case considered in this paper, each of the 113 weather maps contains 84 points. Each of these points contains two observations. This makes 18,984 pieces of data for only two months. Attempts have often been made to find a relatively small set of numbers that contained almost as much information as the original data. This is sometimes done by expressing the data in terms of various linear combinations, since observations at different points are usually correlated with each other.

In some of the first studies in statistical weather prediction, Malone and Miller [3] reduced the number of predictors from 182 to 32 by means of the normalized coefficients (Z's) of 14 Tschebyscheff orthogonal polynomials. However, it appeared in this study that certain Z's were highly correlated with each other when considered as functions of time. Therefore another method was needed in order to represent the maps by a small number of quantities having coefficients uncorrelated with each other.

A method using empirical orthogonal functions (hereafter denoted as EOF) was developed and described by Lorenz [1].

The surface pressure field was expressed as a sum of products of EOF's of time, Q's, and EOF's of space, Y's. The EOF's have these properties:

1. The functions of time, Q's, are orthogonal to each other.

2. The functions of space, Y's, are orthogonal and are chosen in such a way that the sum of the squares of the functions are unity; i.e. they form an orthonormal set.

It was found that 91% of the variance of surface pressure observations at 64 stations over a period of 140 days was represented by only 8 EOF's while 97% of the variance was represented by 16 EOF's.

The computational procedure for determining Y's and Q's was described by Lorenz [1], and applied to prediction of the sea-level pressure field by Shorr [2] and the upper level vorticity field by Sellers [3].

Some of the results from this method will be presented in this paper. The possibility of further improvement of surface pressure prediction by using upper level height data and vorticity data is the principal subject of this study.

II. THEORY AND APPLICATION

1. The Linear Regression Formula

The regression equation for computing a predictand x_0 as a linear combination of predictors $x_1, x_2, \ldots\ldots x_M$ is given by the expression,

$$\hat{x}_0 = \sum_{m=1}^{M} a_m x_m$$

or

$$x_0 = \hat{x}_0 + e_0 \qquad (1)$$

where e_0 is the error in estimating x_0, provided that the time-means of $x_0 \ldots\ldots x_M$ are zero. The coefficients a_m are found by minimizing the mean square of errors. Thus for M = 1,

$$\frac{\partial}{\partial a_1} \overline{e_0^2} = -2\,\overline{x_0 x_1} + 2a_1 \overline{x_1^2} = 0$$

and

$$a_1 = \frac{\overline{x_0 x_1}}{\overline{x_1^2}} \qquad (2)$$

Here a bar indicates an average with respect to time. The expression in the numerator is the covariance of the functions x_0 and x_1. The denominator is the variance of the function x_1. Generally, for m = M, the coefficients a_M are evaluated by the expression given in matrix form

$$(a_1\, a_2 \ldots\ldots a_M) = (\overline{x_0 x_1}\ \ \overline{x_0 x_2} \ldots \overline{x_0 x_M}) \begin{pmatrix} \overline{x_1^2} & \overline{x_1 x_2} & \ldots\ldots & \overline{x_1 x_M} \\ \overline{x_2 x_1} & \overline{x_2^2} & \ldots & \overline{x_2 x_M} \\ \vdots & \vdots & & \vdots \\ \overline{x_M x_1} & \overline{x_M x_2} & & \overline{x_M^2} \end{pmatrix}^{-1} \qquad (3)$$

The second matrix on the right side of (3) is the inverse covariance matrix which has diagonal elements as variances and non-diagonal elements as covariances.

In this study the predictands are 14 EOF's, $q_1, q_2, \ldots\ldots q_{14}$. The predictors are values of these same EOF's at earlier times. If the values of the EOF's at time n-2 alone are used to predict the EOF's at time n, the prediction formula may be written

$$\hat{Q}_n = Q_{n-2} P_1 \qquad (4)$$

when

$$Q_n = (q_1, q_2, \ldots\ldots, q_{14})_n$$

is a matrix of one row and 14 columns, and P_1 is a 14 x 14 matrix of prediction coefficients. The subscript n refers to the time. If the values of the EOF's at times n-2 and n-3 are used as predictors, the formula may be written

$$\hat{\hat{Q}}_n = Q_{n-2} P_2 + Q_{n-3} P_3 \qquad (5)$$

The coefficients in P_1, P_2, and P_3 may be found by solving equations

of the form of (3) for each predictand separately.

Equations (4) and (5) will be used for the surface pressure predictions.

2. The Barotropic Vorticity Equation

The hypothesis was made that the prediction obtained by the statistical method that used only surface pressure data would fail mostly at the pressure centers. Therefore it was thought that an improvement would be made after adding the vorticity data to the prediction formula of surface pressure. The test was made under the assumption of the validity of the barotropic vorticity equation for a two-dimensional non-divergent flow

$$\frac{\partial \zeta}{\partial t} = - \vec{V} \cdot \nabla_p \zeta \qquad (6)$$

In this equation ζ is the vertical component of the relative vorticity, $\vec{V}$ is the horizontal velocity vector and ∇_p is the horizontal del-operator taken with respect to a constant pressure surface. represents the local time rate of change of the relative vorticity and therefore denotes the accumulation of vorticity within a certain unit area. The term on the right side of (6) is the horizontal advection of vorticity through the boundary of the same area.

For many purposes it is useful to use the geostrophic approximation and compute the vorticity from the geostrophic wind.

The geostrophic vorticity, ζ_g , is obtained from

$$\zeta_g = \frac{g}{f} \nabla^2 H + u \frac{\beta}{f} \tag{7}$$

Here g is the acceleration of gravity, f is the coriolis parameter, $\nabla^2 H$ is the Laplacian, $\mathcal{L}$, of the contour field, u is the zonal wind component and β is the Rossby parameter equal to $2\Omega \cos\varphi R^{-1}$. R is the distance from the center of the earth to the surface at latitude φ . R decreases slightly from the equator (6.378×10^6 km) to the poles (6.357×10^6 km). Ω is the angular speed of the earth's rotation (7.292×10^{-5} sec^{-1}). Since the second term in (7) is negligible compared to the first one, it may be omitted. Therefore the geostrophic vorticity is obtained by computing the Laplacian of the 500 mb height. Thus

$$\zeta_g = \frac{g}{f} \nabla^2 H = \frac{g}{f} \mathcal{L} \tag{8}$$

3. The Finite Difference Approximation

The well known finite difference scheme is shown in Fig. 1 for the point i,j. Let the x axis be in direction of the grid rows and the y axis be in the direction of the grid columns.

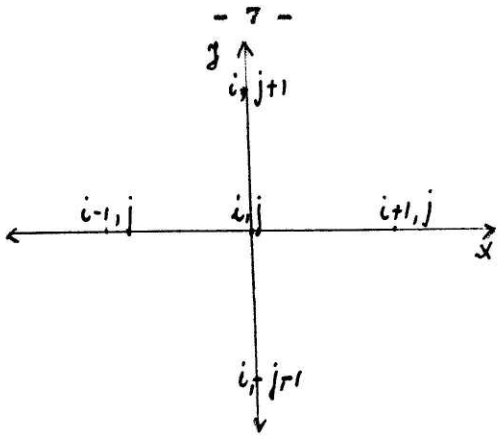

Fig. 1. Finite difference scheme

Here the measurements of the derivatives of the continuous variables x and y are replaced by a discrete set of points (i,j) along the x and y axes respectively. So $x = i\Delta x$ and $y = j\Delta y$ when Δx and Δy are the distances between successive points and i and j have only integer values. Usually the distances between Δx and Δy are equal and are often designated by d. Thus the Laplacian is evaluated as

$$\mathcal{L} = d^{-2}\left(H_{i+1,j} + H_{i,j+1} + H_{i-1,j} + H_{i,j-1} - 4H_{i,j}\right) \quad (9)$$

A problem which always appears is one of choosing distance d. This problem has been discussed by many authors. According to Charney and Phillips [5], one obtains the best results by choosing d = 300 km. This choice depends upon the size of the disturbances that are to be considered.

An attempt was made here to adapt d to the available data so that $\mathcal{L}$ could be easily evaluated. Usually data are available at

latitude and longitude intersections. Therefore d was chosen to equal 5° longitude. However, in such a case, d varies with latitude; also, the distance along the x axis differs from that along the y. Let the distance between i + 1 and i - 1 be d_x and the distance between j + 1 and j - 1 be d_y. Then we define

$$\varepsilon = \frac{d_x}{d_y} \tag{10}$$

The relative vorticity according to (8) is

$$\zeta_g = \frac{g}{f d_x^2}\left[\left(H_{i+1,j} + H_{i-1,j} - 2H_{ij}\right) + \varepsilon^2\left(H_{i,j+1} + H_{i,j-1} - 2H_{ij}\right)\right] \tag{11}$$

Once ζ_g is evaluated, the vorticity equation (6) can be applied by various methods.

In agreement with the vorticity equation, the Laplacian of height change is

$$\nabla^2\frac{\partial H}{\partial t} = -\left(\frac{\partial H}{\partial x}\frac{\partial \zeta}{\partial y} + \frac{\partial H}{\partial y}\frac{\partial \zeta}{\partial x}\right) = -J(H, \zeta_g) \tag{12}$$

where J is the Jacobian determinant of H and ζ_g. At the point i,j,

$$J_{i,j}(H,\zeta) = \left(H_{i+1,j} - H_{i-1,j}\right)\left(\zeta_{i,j+1} - \zeta_{i,j-1}\right) - \left(H_{i,j+1} - H_{i,j-1}\right)\left(\zeta_{i+1,j} - \zeta_{i-1,j}\right) \tag{13}$$

Here the velocity V is expressed by means of the gradient of height in the x and y directions.

Thus equation (6) can be written

$$\frac{\Delta \zeta_g}{\Delta t} = - \frac{g}{f dx dy} J(H, \zeta_g) \tag{14}$$

where the symbol Δ replaces the continuous independent variables of vorticity and time change by the discrete variables according to the finite difference procedure.

To solve equation (12), we should, ideally, invert the Laplacian by relaxation or some other method. However, this equation can be used for forecasting purposes by making the first approximation that the local rate of height change is proportional to its Laplacian. Thus

$$\frac{\partial H}{\partial t} \approx c \nabla^2 \frac{\partial H}{\partial t} \tag{15}$$

The coefficient of proportionality c must be negative and evaluated empirically by correlating values $\frac{\partial H}{\partial t}$ and $\nabla^2 \frac{\partial H}{\partial t}$.

4. The Trajectory Method for Advecting the Vorticity Field

The trajectory of the air parcel, the curve described by the successive position of the parcel during a time interval $t_1 - t_o$, can be expressed as a vector $\vec{T}$,

$$\vec{T} = \int_{t_o}^{t_1} \vec{V}(x, y, p, t)\, dt \tag{16}$$

where $\vec{V}$ is the velocity vector which can be determined for each infinitesimal increment of time. Certainly, such a method in practice must be replaced by some successive approximations where the vector $\vec{V}$ is known at the beginning and end of each time interval Δt. Since the upper level charts in our case are available every 24 hours, the method represents only a very rough approximation.

We shall make two assumptions: (1) the trajectories coincide with the streamlines initially, and the velocity of the parcel is constant and is determined by the wind field at the beginning of the time interval. (2) the air parcel remains on the same pressure level $\vec{V} = \vec{V}(x,y,t)$. (A convenient method for evaluating the geostrophic wind is described by Pettersen [7]).

Trajectories can be evaluated for a selected number of points by using these points as the final positions of trajectory vectors. Here $\vec{V}$ is taken at each selected point as the first approximation and then corrected by using its mean value along the whole trajectory. The value of vorticity at the origin point of the trajectory is used as the predicted vorticity at the end of the trajectory (applied in section III, 2b).

Synoptic experience shows one that better results are obtained when complete vorticity isopleths are advected and when we use for the initial position of trajectory a selected number of intersections of vorticity and contour lines (section III, 3b).

Assuming the conservation of the absolute vorticity, the vorticity forecast for the time interval Δt is obtained here by displacing the vorticity contours over a distance $\vec{V}\Delta t$. Here the question arises as to how conservative the field $\vec{V}$ is during the time interval Δt. Fjortoft [8, 9] has shown that better solutions can be obtained if the advective field $\vec{V}$ is replaced by a more conservative field which would be found by some smoothing process.

5. Data and Procedure

The experiment was made at a grid of 84 points over the United States, Southern Canada and parts of the surrounding oceans. The 113 maps of 24-hour difference were considered from January 3 to February 28 at 0030 and 1230Z.

These maps were compared with daily weather maps of January and February 1951 [10]. 56 maps at 24-hour intervals from January 3 to February 27 at 1230Z were compared with upper level maps. From this group, the first 31 maps were compared also with vorticity. For upper level data, 500-mb charts were chosen. The values of heights for the whole January, February 1 and February 2 were read off at 150 points of latitude-longitude intersections (20 - 65°N, 60 - 130°W) from daily weather maps [10] at 1530Z. Then these maps were analysed. Heights were evaluated in tens of feet, and contours were drawn at intervals of 200 feet. From these maps vorticities were obtained for 42 grid

points using equation (11). The units are 10^{-5} sec^{-1}. As mentioned earlier, the corrections had to be made for each latitude for quantities ϵ , f and d_x . The values of d_x were read off from Lambert Conformal Conic Projection Maps with Standard Parallels 30° and 60° and the map scale 1 : 13,000,000. One latitude degree of this map at 30°N represents 60 nm = 111 km. For example d_x for 50°N was evaluated as 3.6° longitude at 30°N which is 400 km. The values d_x for other latitudes are tabulated in column 2 of Table 1. In column 3 of this table are the values for ϵ^2 and in column 4 is $\frac{g}{f}\frac{1}{d_x^2}$

$\phi^{\circ}N$	$f\ 10^{-4}$	d_x km	ϵ^2	$\frac{g}{f}\frac{1}{d_x^2}$
60	1.263	300	0.232	0.862
55	1.194	361	.336	.629
50	1.117	400	.413	.548
45	1.031	433	.484	.507
40	.937	477	.588	.460
35	.836	522	.704	.430
30	.729	555	.796	.436
25	.616	588	.893	.460

Table 1. The values for the Coriolis parameter f distance d_x , and constants ϵ^2 and $\frac{g}{f}\frac{1}{d_x^2}$ for different latitudes.

Vorticity data were analysed on the same maps with 500-mb contours. The first attempt was made by computing the vorticities

at each of the 64 points. The isopleths were so irregular that it was necessary to do some sort of smoothing. It seemed that it was better to obtain the vorticity field at 42 points only and then to interpolate for the rest of the points. In figures 22 and 23 are the selected 42 points from which the vorticities were computed.

The 500-mb heights from February 3 - 27 at 1530Z for each 5° latitude and 10° longitude from 25° - 55° and 70° - 120°W were available from the M.I.T. General Circulation Project.

The vorticity was computed by a desk calculator, whereas the statistical procedures were programmed by Prof. Lorenz for computation by the LGP-30 electronic computer of the Statistical Forecasting Project at M.I.T.

III. RESULTS AND COMMENTS

1. Surface Pressure Prediction Maps

Surface pressure prediction was made for a 24-hour time difference. All maps were expressed by means of 14 empirical orthogonal functions. According to equations (4) and (9), two predictions were made: (1) one contained only one term (equation (4)) (hereafter called "one-map prediction"). That means the prediction formula contains only the data at lag-1, i.e. 24 hours previously. (2) the other contained two terms (equation (9)) ("two-map prediction") where the first predictor at lag-1 is 24 hours and the second at lag-2, 36 hours previously. All these past data were used at the same points for which the prediction was made.

As expected, on the average, better results were obtained by using the two-map prediction than the one-map prediction. The estimates of error were made by comparing the results with climatology and persistence predictions. Climatology prediction means that the prediction map is simply the average monthly map. Persistence means that the pressure is assumed to be the same as it was 24 hours earlier at the same points. The errors were expressed as the sum of the square of errors over all points. Thus

$$E = \sum_i e_i^2 \qquad (17)$$

The Table 5 in Appendix I shows these errors. The prediction is assumed to be good if the error is at least twice as small as the one obtained

by climatology. The largest errors which were on February 1 and February 2 will be discussed later. Comparison of all errors obtained by statistics and persistence was made with those obtained by climatology. The reduction of error RE with respect to climatology was computed by the formula,

$$RE = 1 - \frac{E}{E_c} \tag{18}$$

where E_c is the climatology error. All errors are expressed by (17). Column 5 in Table 5 represents the reduction of error for persistence (RE_p), column 6 is the reduction of error for the one-map prediction (RE_{1m}) and column 7 is the reduction of error for the two-map prediction (RE_{2m}). Obviously the prediction for both the 1-and 2-map prediction is very good in comparison to the persistence. The average reduction of errors $\overline{RE}_p = .12$, $\overline{RE}_{1m} = .63$ and $\overline{RE}_{2m} = .70$. The averages $\overline{\overline{RE}}_p = -.87$, $\overline{\overline{RE}}_{1m} = .54$ and $\overline{\overline{RE}}_{2m} = .61$ if the reductions of errors for each day separately are averaged. From the 113 maps, 49 RE_p's and 5 RE_{2m}'s were negative. Upon comparing the reduction of error with column 1, it was seen that the negative RE's for all of the three predictions at the periods January 4 - 5, February 4 - 5 and February 20 - 21 were due to the relatively low error of climatology. The largest errors during the period January 15 - 17 appear at the same time as the largest errors of climatology.

Special investigation was made of the maps for January 4, 5, 10, 12, 20 and February 1 and 2 at 1230Z for which the upper level and vorticity maps were available.

2. Test of Improvement of the Two-Map Prediction Formula by 500-mb Vorticity and Height.

a. Test with observed values.

In order to see if there is any possibility for improving the surface pressure prediction by vorticity data, the test was made at first with observed values. The vorticity field was analysed for the maps with the 500-mb contour field. The positive isopleths indicate the cyclonic vorticity and the negative ones the anticyclonic vorticity. As can be seen from the maps, the zero lines pretty well separate the 500-mb troughs from the ridges.

Rough qualitative comparison of the vorticity maps with the 24-hour surface pressure change shows that the pressure fall corresponds to the advection of cyclonic vorticity (positive values) while the pressure rise corresponds to the advection of anticyclonic vorticity (negative values). Point by point a comparison was made between the 500-mb height and the vorticity maps and also between the 24-hour height change and the vorticity change. It turns out that the largest error in surface pressure prediction comes mostly from poor prediction of the pressure center's intensification.

Let us now consider the situation of January 4 which was among the poor predictions. Figure 2 shows a two-map prediction pressure field. In this map, the pressure trough was predicted in the direction SW-NE from 30°N 105°W to 45°N 85°W. Going back to the vorticity map of January 3, (Fig. 3) it is found that a strong cyclonic vorticity at 40°N 95°W is situated in the upper level trough. After a rough qualitative estimation at the 500-mb chart of January 3, it was expected that the trough will move eastward together with the cyclonic vorticity. According to the gradient at the 500-mb level the displacement was estimated at about 15° - 20° longitude. If the hypothesis is true that the cyclonic vorticity advection, accompanied by height fall, indicates the surface pressure fall, then the cyclone's center should be expected to move eastward and probably be deeper than predicted. Also the cyclonic vorticity is expected to be replaced by anticyclonic vorticity as well as to be accompanied by height and pressure rise in the region about 30°N 95°W. The maps of verification (Fig. 4) show that the above hypothesis was correct. Figure 5 shows the vorticity map on January 4 at 1530Z. Here the cyclonic vorticity center was displaced 20° eastward at 45°N 75°W while around the region 30°N 95°W the cyclonic vorticity was replaced by anticyclonic vorticity. The 24-hour vorticity change and the 24-hour 500-mb height change (hereafter called vorticity change and height change, respectively) also show a good agreement with the hypothesis. The comparison was made between the prediction map in Fig. 2 and the verification map in Fig. 4 on January 4. Point by

point, errors in mb (Fig. 6) were found for 42 grid points. These maps will be called error maps .

In order to obtain some quantitative results for what was established qualitatively, three methods were tested for the same situation and also were applied to other situations with larger statistical errors. These methods are as follows:

Method A_o . The analysis of the January 4th situation promised good prediction when adding the vorticity values, multiplied by some coefficient, to the pressure prediction map. Rough estimation made by comparing the error map with the verification map suggested the use of the coefficient of magnitude .5 which, established theoretically, must have the negative sign. This method is called A_o , where subscript o should distinguish this method obtained by observed values from the same method where the vorticity will be predicted. The results for selected dates are shown in Table 2. The errors in the first columns are defined as the sums of the absolute values of the errors for each point. The numbers in the second part of each column are the reduction of error in this test. They are expressed by the formula

$$RE = 1 - \frac{\Sigma |e|}{\Sigma |e|_s} \qquad (19)$$

where $\Sigma |e|_s$ is the statistical error and where $\Sigma |e|$ is the error of the particular method used and will have the subscript according to the method.

Date	Jan. 4		Jan. 5		Jan. 10		Jan. 12		Jan. 20		Feb. 1		Feb. 2		Average	
Method	$\Sigma\|e\|$	$R\varepsilon$	$\Sigma\|e\|$	$R\varepsilon$	$\Sigma\|e\|$	$R\varepsilon$	$\Sigma\|e\|$	$R\varepsilon$	$\Sigma\|e\|$	$R\varepsilon$	$\Sigma\|e\|$	$R\varepsilon$	$\Sigma\|e\|$	$R\varepsilon$	$\Sigma\|e\|$	$R\varepsilon$
S	177		157		151		137		181		261		246		188	
A_o	155	.12	233	-.48	159	-.01	180	-.31	198	-.09	315	-.20	363	-.48	229	-.22
B_o	145	.18	179	-.14	165	-.05	115	.16	173	.04	275	-.05	247	.00	186	.01
C_o	145	.18	141	.10	161	-.03	134	.02	142	.22	295	-.13	223	.09	177	.06
r_{BC}		-.73		-.07		-.78		-.67		-.20		-.61		-.49		

Table 2. Errors in prediction by the statistical (S), vorticity (A_o), change of vorticity (B_o), and change of 500-mb heights (C_o) methods. r_{BC} is the correlation coefficient between vorticity change and height changes at 42 points.

The results for method A_o in Table 2 are pretty discouraging, since they show that only the first situation examined gives better results and accurate corrections. Considering the results for January (Table 6, Appendix I), it is seen that this is at the same time the only case in the whole month in which method A_o gives a smaller error than method S. The average reduction of error due to the statistical method is -.39 .

Some investigations show that a few of the predictions failed only in the intensity of the pressure centers, but the prediction of pressure patterns was correct. Rough tests were made to find out if improvement could be obtained by adding the vorticity either to the centers only, or to both the center and surrounding points. The results indicated that such an improvement could be possible, but that the coefficient would have to be changed for each situation and should be found empirically. (For example, for January 15, 21, 22 and 27, the coefficients .5, .9, .7 and .4, respectively, give the best results for the correction of the pressure centers.) However, intuitively, only a slight improvement could be obtained in this way. One should especially keep in mind that the above experiment was made by observed data and also that the predicted vorticity would contain some prediction errors.

Method B_o. In seeking some other method which would have brought forth better results than the vorticity field, an attempt was made to use the vorticity change instead of the vorticity itself. The 24-hour vorticity change was used at the same 42 points and was multiplied by the coefficient .2 which was found again empirically. These results are shown in the third row of Table 2. Except for one case, results were better than those obtained by the A_o method. In comparison to the statistical method there was only a slight improvement. However, the results obtained for the whole month (Table 6, Appendix I) don't show any improvement over the statistical method and are even slightly

poorer (-.06). The test was again made by using a different coefficient, but the results were poor and did not promise much improvement.

Method C_o. As a further step, the comparison was made between height change and vorticity change; according to equation (15), the Laplacian of the height change could be approximated by the height change at the central point. If this hypothesis is correct the correlation between the height change and the vorticity change might give high negative values. In case of positive results the entire procedure could be simplified, since the vorticity would be eliminated and then only heights would be needed.

The results that were found when the height change was multiplied by the coefficient .1 are shown in Table 2. Except for two cases, the results were better than those obtained by statistics; and some improvement is also indicated in the average. The largest difference between the S method and the C_o method was found on February 1; this contributes considerably to the average.

Correlations between change of height and change of vorticity are shown in the last row of Table 2. Comparing them with the results in B_o and C_o methods, it can be seen that the correlation coefficient is not the most suitable quantity for our purpose. However, it does show a picture of connection between the two values in consideration. But, upon applying it to the third quantity as in our case, it cannot give a desirable answer; since it is not possible to see which of the

two compared values is larger in separate cases. In Table 6, it is seen that the results for the whole month indicate a slight improvement by using method C_o over method S. Here the reduction of error was .03.

A reduction of the error .02 is found for all of the 56 maps. However 33 of these maps give better results in method C_o than in the statistical method, whereas the other 23 maps do not show any improvement.

b. Synoptical Statistical Approach to Prediction

The results obtained in previous sections were based on observed vorticities and heights. Now the question is how we can predict the values of vorticity and height which are used in methods A_o, B_o and C_o.

In order to find these predicted values, a more or less synoptical approach was used. However, an attempt was made to symplify the synoptical procedure as much as possible in order that it might be used for statistical purposes later on.

Method A_p and B_p. The subscript 'p' indicates that methods A_o and B_o will be used with the predicted values of vorticity. As mentioned under 2 in section II, in using the barotropic model, it was assumed that the absolute vorticity field was constant. That means that the present vorticity can be advected in some sort of steering flow

for which in this case the 500-mb contour field was chosen. Even though a very rough approximation was made, the 500-mb flow was taken to be constant for each 24-hour time interval.

For this experiment 18 points were chosen (see Fig. 22 in Appendix II) at which the trajectories were found. The assumption was made that the trajectories and the streamlines coincide, as explained in section II, 4. The new vorticity values were then considered as the predicted vorticities for the next day at these same points. Obviously, the error could be considerably larger if the upper level pattern varied rapidly. The predicted values of vorticity were multiplied by the same coefficient -0.5, as in A_o, and added to the statistical results in S.

For method B_p, corresponding to method B_o, the changes of vorticity were taken as differences between predicted values on one day and observed values on the previous day. These differences were multiplied by the factor -0.2. The methods A_p and B'_p were applied to the same situation as those in Table 2 and are shown in Table 3. Here the statistical values are the same as in Table 2, only they are taken over 18 points as in methods A_o and B_o. Upon comparing the corresponding errors in Tables 2 and 3, it is seen that on the average, they turn out to be almost the same. However, in comparing the situation day by day, it was noticed that the predictions by both A_p and B_p for February 1 and February 2 gave better results than A_o and B_o.

Date	Jan. 4		Jan. 5		Jan. 10		Jan. 12		Jan. 20		Feb. 1		Feb. 2		Average	
	$\Sigma\|e\|$	RE	$\Sigma\|e\|$	RE	$\Sigma\|e\|$	RE	$\Sigma\|e\|$	RE	$\Sigma\|e\|$	RE	$\Sigma\|e\|$	RE	$\Sigma\|e\|$	RE	$\Sigma\|e\|$	RE
S	86		44		69		52		48		94		130		75	
A_p	82	.05	82	-.86	73	-.06	89	-.71	37	.23	76	.19	126	.03	81	-.08
B_p	80	.07	66	-.50	77	-.11	61	-.17	47	.02	76	.19	119	.09	75	.00

Table 3. The error of prediction of the surface pressure field by statistical (S), vorticity (A_p) and change of vorticity (B_p) methods for 18 points.

In seeking the causes of this fact, unfortunately there are so many possibilities for errors that it would be hard to say which error is ...ling here. Some of the possibilities of errors are: the finite difference approximation procedure for evaluating the vorticity values, the insufficiency of the barotropic model, the 500-mb flow not being stationary and the errors not being obtained from the same number of points, so that the region of the largest error in the first case could be avoided in the second.

It is shown (Table 6) that over the whole month of January that only in 4 cases the A_p method was better than the S method, and that an average reduction of error due to statistics was -.25 . In the B_p method 13 of the 31 cases had better results in the B_p method than in the statistical method. Here the reduction of error was -.05 .

Method C_p . In formula (15), as was said previously, it is assumed that the Laplacian of the change of height could be approximated by the change of height at the central point multiplied by one factor and vice-versa. On this assumption method C_o was made. In order to find the numerical value for the prediction by method C_p ; we will make use of the following approximation,

$$\frac{\partial h_o}{\partial t} = a \frac{\partial H}{\partial t} = b \, J(H, \zeta) \tag{20}$$

where $\frac{\partial h_o}{\partial t}$ is the local surface pressure change, a and b are constants and the other symbols have the same meaning as those in equation (12). That means that the surface pressure prediction could be obtained by determining the Jacobian of height and vorticity at the 500-mb level. This experiment was used to predict the surface pressure for Feb. 2, and the results will be described in the next section.

c. The Period from January 31 - February 2

As can be seen in previous sections, the largest error was found on February 1 and February 2. Now it will be discussed here in more detail. Figures 7 and 8 show the sea-level and the 500-mb level maps, respectively, which are both analysed in tens of feet. A weak sea-level trough between two high centers extends in the SW-NE direction from 105° - 85°W. With a gradual slope, in the same

direction as the sea-level trough, extends the upper level trough. The cyclonic and the anticyclonic vorticity (Fig. 9) agree with the upper level and also with the sea-level pattern. On the surface daily weather maps, the front is seen with a temperature contrast of about 15°F and is situated in the weak trough (shown with the full line in Fig. 7) from 30°N and 95°W to 43°N and 78°W. The temperature contrast in the upper level trough was about 20°F. The rough synoptic estimation of prediction was as follows: both the sea-level and the upper level patterns indicate that the temperature contrast should be stronger because of the advection of warm air in advance of the front and cold air in the rear of the front. In addition to this, the weak cyclone with the center at 25°N and 105°W will move north westward in the strong upper level stream while the anticyclone at 50°N and 120° will move southeastward and be accompanied by the cold advection. Then one could expect the pressure rise in the middle of the map.

Figure 10 shows the sea-level situation of February 1. It is seen already that the qualitative estimation made above was correct and that the synoptic situation developed as was expected. Figures 11, 12, 13, 14 and 15 show the 24-hour pressure change, the two-map prediction by the statistical method, the error map by the two-map prediction, the change of the 500-mb heights and the change of the 500-mb vorticity field, respectively. From the error map it is seen that the statistical method gives too high values of pressure at the upper part of the map and too low values at the lower part of the map. From maps 11, 14 and 15,

it is obvious why the results of methods B_o and C_o in Table 2 were so poor. The height fall and the cyclonic vorticity pattern differed from the low pressure pattern at sea-level by one westward slope and gave at some points the wrong (opposite) corrections to the statistical method (double fall or rise). Better results were obtained by using the trajectory method as described on page 23.

While seeking a method which will give quantitative results for what was described above when considering the cyclogenesis qualitatively, it was supposed that the method should contain the information of temperature either on sea or on upper level maps. Synoptic experience suggested the use of the thickness map analysis. Figure 16 shows the 500/1000 thickness on January 31, 1530Z. Each number is a difference between a 1000-mb and a 500-mb height value. The 1000-mb heights were obtained from the pressure values p_o's by using the formula,

$$H_o \approx 25\,(p_o - 1000) \qquad (21)$$

where H_o's were the 1000-mb heights in feet. It was decided to use a method similar to the previous trajectory method, the difference being that the thickness vorticity isopleths would be advected as a whole instead of point-by-point. The thickness vorticities were obtained in the same way as the 500-mb vorticities. Further, the question was what to use as a steering flow, i.e. how to determine the thickness velocity field. The idea was to obtain a smooth prediction field of

thickness contours as one approximation by using the statistically predicted surface two-map prediction on February 1 (Fig. 12).

Although this two-map prediction was poor for the surface pressure prediction, it was hoped that it would suffice for this thickness prediction. In order to do this, first the two-map prediction for February 1 and the sea-level pressure map for January 31 were expressed as 1000-mb heights (formula 21). Then the predicted 24-hour height change was obtained by taking the difference of these two maps. Finally this predicted map of 1000-mb height change was added to the thickness map for January 31. The whole procedure was done graphically, and the values of the 42 points were read off. The predicted thickness field was then used as a steering flow for the last 12 hours. The following assumptions were made: the wind field is constant for the first 12 hours and is given by the thermal wind at the beginning of the time interval. Then, the velocity changes instantaneously and for the remaining 12 hours is given by the thermal wind at the end of the time interval. The predicted thickness map and the vorticities are shown in Fig. 17. The vorticity values were read off from the graphically obtained field at the 18 points (see Fig. 22). Again the vorticities were multiplied by the coefficient -.5, and were added to the statistical two-map prediction. The sum of the absolute values of error is given in Table 4 and is compared with the statistical values in Tables 2 and 3. Results of method $B\zeta_T$ are given in the third

column of Table 4, i.e. the predicted values of the vorticities for one day were subtracted from the values for the previous day in order to obtain a 24-hour change of vorticity. The result is slightly poorer, but a coefficient of .3 (column 4) instead of .2 indicates the best result obtained by this prediction.

S	$A\zeta_T$ coeff. -.5	$A\zeta_T$ coeff. -.2	$B\zeta_T$ coeff. -.3
94	57	61	53

Table 4. Errors by the thickness method

Figures 18, 19, and 20 show a two-map prediction error map by the statistical method and the 24-hour height changes, respectively, on February 2. As was mentioned earlier the test was made to predict the surface pressure by method C_p. 30 points from 30° - 50°N to 70° - 125°W were chosen (see Fig. 22). For the boundary conditions, vorticities at 17 additional points had to be evaluated. This required 36 additional values of height data. The coefficient b in equation (20) was evaluated empirically as the mean ratio between obtained Jacobians and surface pressure changes. For the above situation, this coefficient turned out to be -0.08. As in previous methods, the Jacobian at each point was multiplied by this coefficient and added to the two-map

prediction. The results were unsatisfactory. $\Sigma|e|$ was 227, whereas the statistical error for the same number of points was 194. The Jacobians were plotted in Fig. 21.

IV. CONCLUSIONS AND SUGGESTIONS FOR THE FUTURE WORK

As was mentioned earlier, the purpose of this work was to investigate the possibility of combining the surface pressure data with the upper level heights and vorticities in order to gain better results for the surface pressure prediction than those obtained by purely statistical methods, using surface data alone.

A test was made to determine whether the vorticity data at the 500-mb level or the 500-mb heights could improve the surface pressure prediction formula. The results are given in Table 5 in Appendix I. They show:

1. In methods A_o and A_p, vorticity values combined with the statistical method show poorer results than statistics alone.

2. The changes of vorticity in methods B_o and B_p show somewhat better results, but the methods still prove poorer than the statistical method alone.

3. Better results than the statistical method alone might be expected by combining the 500-mb height changes and the statistics (method C_o).

The correlations between change of height and change of vorticity suggest the possibility of replacing the vorticity values by upper level heights (Table 2).

As far as prediction is concerned two methods for obtaining the height change are suggested:

1. Apply the same prediction formulae (4) and (5) for 500-mb level data. We noticed that when Sellers applied the EOF's on the vorticity data, he also mentioned in his conclusions that the use of the height as expressed by the empirical functions could be a better predictor of height than the vorticity as a predictor of the heights.

2. Use the formula (15) for obtaining the height change instead of the surface pressure change as in formula (20). Determine the coefficient c for the whole month, but for each latitude separately. It is suggested that one apply the formula (15) for a 12-hour interval and then use this prediction as a steering flow for the next 12-hour interval in order to obtain the 24-hour prediction.

The investigation of the situation of February 1 suggests these additional experiments:

1. Make correlations between the prediction error and either the sea-level or some upper level temperature field.

2. Apply the formula (20) to the 500/1000-mb thickness charts instead of to the 500-mb charts.

Finally, experiments could be made by using the sea-level vorticity together with the divergence field. Certainly, this would make the entire procedure much more complicated, since the divergence must be evaluated from the observed winds at station networks.

ACKNOWLEDGMENTS

I wish to express my deepest appreciation to Prof. Edward N. Lorenz for his assistance and advice during the work on this study. I acknowledge the stimulating and helpful discussions with Mr. J. O. Ellis. Thanks are extended to Dr. B. Saltzman from the M.I.T. General Circulation Project for making available the 500-mb data. I am very indebted to Mrs. M. Hamilton for her help in reading the manuscript and in the preparation of this thesis. Thanks are due to Miss M. L. Guillot for typing the manuscript, and to Mrs. G. Taft and Miss L. Blake for typing tables and figures.

In addition, I wish to express my gratitude to the members of the staff of the M.I.T. Meteorology Department who made it possible for me to come to M.I.T., as well, who during my stay helped, discussed with and encouraged me in my work and study.

REFERENCES

1 Lorenz, E.N., 1959: Project of statistical weather forecasting final report of Statistical Forecasting Project, M.I.T., pp. 1-78.

2 Shorr, B., 1959: Empirical orthogonal functions applied to the prediction of the sea-level pressure field, Project for Statistical Weather Forecasting. Final report of Statistical Forecasting Project, M.I.T., pp. 79-143.

3 Sellers, W.D., 1957: A statistical dynamic approach to numerical weather prediction, Statistical Forecasting Project, M.I.T. Scientific report No. 2.

4 Miller, R.G., and T.F. Malone 1956: The application of synoptic climatology to the prediction of sea-level circulation patterns. Studies in synoptic Climatology, Cambridge, Mass, final report of Synoptic Climatology Project, M.I.T.

5 Charney, J.G. and N.A. Phillips, 1953: Numerical integration of the quasi-geostrophic equations for barotropic and simple baroclinic flow, J. Meteor., 10, 71-99.

6 Phillips, N.A., 1956: The general circulation of the atmosphere: a numerical experiment, Quaterly Journal, 82, April, 1956.

7 Pettersen S., 1956: Weather analysis and forecasting, volume I: numerical forecasting, graphical integration pp 371-402; computation of winds, p. 412.

8 Fjortoft, R., 1952: On a numerical method of integrating the barotropic vorticity equation, Tellus, Vol. 4, No. 3.

9 Fjortoft, R., 1955: On the use of space smoothing in physical weather forecasting, Tellus, Vol. 7, No. 3.

10 Daily series synoptic weather maps northen hemisphere sea-level and 500-millibar charts January and February 1951, U.S. Weather Bureau.

APPENDIX I

Table 5. The errors in the statistical methods and the C_o method.

DATE	GMT	E_c	E_p	E_{1m}	E_{2m}	RE_p	RE_{1m}	RE_{2m}	S	RE_{c_o}
Jan. 3	0030	4595	2444	3267	3103	.47	.29	.32		
	1230	3296	1645	1381	561	.50	.58	.83	119	-.21
Jan. 4	0030	1871	3020	1421	2114	-.65	.22	-.15		
	1230	1011	2396	1046	964	-1.16	-.04	.13	177	.18
Jan. 5	0030	709	2089	734	570	-1.96	-.04	.19		
	1230	923	2673	1130	1211	-1.90	-.23	-.31	157	.09
Jan. 6	0030	2307	2852	1516	765	-.24	.34	.67		
	1230	3401	1930	1535	565	.43	.55	.83	116	.22
Jan. 7	0030	3285	1448	667	296	.56	.80	.91		
	1230	3034	1469	736	691	.52	.76	.77	138	.25
Jan. 8	0030	2453	2622	1010	1023	-.17	.59	.58		
	1230	3383	4516	1044	683	-.33	.58	.80	115	-.35
Jan. 9	0030	3144	3984	761	334	-.26	.76	.89		
	1230	3297	3483	501	701	.06	.85	.79	123	-.20
Jan.10	0030	2180	1512	590	437	.30	.73	.80		
	1230	1823	1636	1095	947	.10	.40	.48	157	-.03
Jan.11	0030	1657	1248	763	504	.25	.54	.70		
	1230	2612	2241	883	601	.14	.66	.77	121	.10
Jan.12	0030	2219	1743	747	669	.22	.67	.70		
	1230	1092	1915	1156	898	-.75	-.06	.18	137	.02
Jan.13	0030	1174	1848	1001	686	-.57	.15	.42		
	1230	1621	1470	684	580	.09	.58	.64	136	.19
Jan.14	0030	2221	1717	692	808	.24	.69	.74		
	1230	2453	2109	432	482	.14	.82	.80	111	.05
Jan.15	0030	3149	4333	1217	1200	-.38	.61	.62		
	1230	6517	6725	2863	1946	-.03	.56	.70	198	.30
Jan.16	0030	9083	6211	3503	2541	.23	.51	.69		
	1230	8552	5524	1525	660	.35	.82	.92	134	-.38
Jan.17	0030	7962	4147	1378	1049	.48	.83	.87		
	1230	10252	3494	2991	3132	.66	.71	.69	274	-.09
Jan.18	0030	7775	1513	488	224	.81	.94	.97		
	1230	5090	2170	462	360	.57	.91	.93	104	.12
Jan.19	0030	3173	2541	369	393	.20	.88	.88		
	1230	2266	2253	358	488	.01	.84	.79	107	.18

APPENDIX I (2)

DATE	GMT	E_c	E_p	E_{1m}	E_{2m}	RE_p	RE_{1m}	RE_{2m}	S	$R\varepsilon c_o$
Jan.20	0030	1876	3138	1221	966	-1.27	.12	.30		
	1230	2177	4905	2383	1352	-1.25	-.09	.38	181	.22
Jan.21	0030	3394	3891	1968	961	-.14	.42	.72		
	1230	4356	6008	1963	1644	-.38	.55	.62	163	-.21
Jan.22	0030	3476	5887	923	867	-.70	.73	.75		
	1230	2794	6623	667	442	-1.37	.76	.84	92	-.02
Jan.23	0030	2228	6168	479	339	-1.76	.78	.85		
	1230	2189	3470	1114	1091	-.59	.49	.50	155	.19
Jan.24	0030	1856	1720	1500	1584	.08	.20	.15		
	1230	1798	3140	942	715	-.74	.48	.60	111	.18
Jan.25	0030	1843	3199	239	421	-.74	.87	.77		
	1230	2261	1122	697	649	.50	.70	.71	133	.07
Jan.26	0030	2280	771	870	531	.66	.62	.77		
	1230	2336	1143	998	492	.51	.57	.79	112	-.27
Jan.27	0030	3452	2010	2188	960	.42	.36	.28		
	1230	3811	2326	1487	685	.39	.61	.82	138	-.22
Jan.28	0030	4913	1376	1133	1005	.72	.77	.79		
	1230	5794	2403	1445	1611	.58	.75	.72	193	.12
Jan.29	0030	6917	2118	993	868	.69	.86	.87		
	1230	6554	1076	555	454	.83	.91	.93	115	.16
Jan.30	0030	5502	893	536	736	.84	.91	.87		
	1230	5922	597	466	815	.90	.92	.84	125	.02
Jan.31	0030	5908	1342	881	1067	.77	.85	.82		
	1230	5374	1444	725	617	.73	.86	.88	130	.06
Feb.1	0030	3231	3110	1424	1318	.06	.56	.59		
	1230	3348	8428	3536	2258	-1.52	-.06	.32	261	.13
Feb.2	0030	3733	2232	1322	2478	.40	.65	.34		
	1230	5156	2073	1260	2150	.60	.76	.59	246	.09
Feb.3	0030	4017	5714	2300	3368	-.42	.43	.16		
	1230	3119	3201	1416	1825	-.03	.54	.41	238	.08
Feb.4	0030	1033	3433	1712	1185	.67	.83	.12		
	1230	1021	4164	1882	1109	-3.08	-.84	.09	167	.13
Feb.5	0030	1009	1625	876	289	-.61	.13	.71		
	1230	1457	1557	876	565	-.07	.40	.61	116	.03
Feb.6	0030	2343	1890	847	557	.20	.64	.76		
	1230	3161	3710	908	755	.17	.71	.76	144	.04

APPENDIX I (3)

DATE	GMT	E_c	E_p	E_{1m}	E_{2m}	RE_p	RE_{1m}	RE_{2m}	S	$R\varepsilon c_o$
Feb.7	0030	2819	4527	1087	911	.60	.61	.68		
	1230	3049	7754	1361	816	-1.53	.56	.73	139	.14
Feb.8	0030	3922	8311	1453	1258	-1.12	.63	.68		
	1230	3137	4032	1741	1451	-.28	.45	.54	169	-.06
FEb.9	0030	2233	3098	1715	1716	-.39	.23	.28		
	1230	2779	4419	1216	895	-.59	.57	.68	152	.16
Feb.10	0030	3248	4398	810	807	-.35	.75	.75		
	1230	4300	3578	1477	968	.17	.66	.77	158	.22
Feb.11	0030	2715	2944	975	847	-.08	.64	.69		
	1230	1634	4200	677	699	-1.57	.58	.59	138	-.07
Feb.12	0030	1269	2787	621	306	-1.19	.51	.24		
	1230	1467	2245	765	796	.53	.48	.46	128	-.06
Feb.13	0030	2572	2432	1095	897	.06	.57	.65		
	1230	3954	4083	1755	1213	-.03	.55	.69	180	.08
Feb.14	0030	5106	6279	2046	1227	-.23	.60	.76		
	1230	6015	3779	1321	356	.37	.78	.94	92	-.34
Feb.15	0030	5596	1719	1489	1046	.69	.73	.21		
	1230	5199	1807	1516	1218	.65	.71	.77	182	.02
Feb.16	0030	3811	2573	913	868	.67	.76	.77		
	1230	2625	2172	803	718	.18	.70	.73	151	-.03
Feb.17	0030	1537	1495	269	231	.03	.82	.85		
	1230	1601	1085	751	589	.32	.53	.37	122	-.14
Feb.18	0030	1900	871	981	560	.54	.51	.71		
	1230	1625	700	605	331	.57	.63	.80	90	.07
Feb.19	0300	1803	1101	487	268	.39	.73	.85		
	1230	1207	1046	400	393	.13	.67	.68	102	-.01
Feb.20	0030	786	1340	337	309	-.70	.57	.61		
	1230	387	1173	451	620	-2.00	.15	.59	125	-.22
Feb.21	0030	666	1229	1073	739	-.84	.60	.11		
	1230	1599	2271	1549	1337	-.41	.03	.14	168	.23
Feb.22	0030	2579	2345	1323	907	.09	.49	.65		
	1230	2842	2450	770	555	.14	.73	.80	131	.06
Feb.23	0030	3069	1691	1280	1217	.45	.58	.60		
	1230	2647	1651	862	917	.38	.68	.65	162	.15
Feb.24	0030	2112	2783	1468	1780	-.31	.30	.16		
	1230	2116	2355	1608	934	-.11	.24	.56	143	-.01
Feb.25	0030	2349	1312	1979	1397	.44	.16	.40		
	1230	2185	1298	1742	947	.41	.21	.57	168	.24

APPENDIX I (4)

DATE	GMT	E_c	E_p	E_{1m}	E_{2m}	RE_p	RE_{1m}	RE_{2m}	S	$R\mathcal{E}c_o$
Feb.26	0030	2426	1647	1075	317	.32	.56	.87		
	1230	2423	2225	1159	842	.08	.52	.65	142	.01
Feb.27	0030	2900	1411	859	647	.51	.70.	.78		
	1230	2614	1504	422	497	.43	.84	.80	115	-.01
Feb.28	0300	3103	1523	706	571	.51	.77	.82		
	1230	2572	2979	1940	1859					
Average:		3138	2783	1165	945	-.87	.54	.61	146	.02
R E:			.12	.63	.70					

APPENDIX I

Table 6. Some of the absolute values of errors by the different methods.

DATE	S	A_o	B_o	C_o	S	A_p	B_p
Jan. 3	119	204	161	144	57	82	72
Jan. 4	177	1551	145	145	86	82	80
Jan. 5	157	233	179	141	44	82	66
Jan. 6	116	142	134	90	37	66	55
Jan. 7	138	147	125	103	70	74	67
Jan. 8	115	213	151	155	46	73	58
Jan. 9	123	167	132	148	67	86	59
Jan.10	157	159	165	161	69	73	77
Jan.11	121	202	132	109	31	53	47
Jan.12	137	180	115	134	52	89	61
Jan.13	136	176	136	110	58	77	52
Jan.14	111	190	112	105	30	45	25
Jan.15	198	236	173	139	83	72	74
Jan.16	134	175	184	185	56	66	58
Jan.17	274	302	298	299	83	91	110
Jan.18	104	149	121	91	36	41	50
Jan.19	107	174	104	88	45	90	46
Jan.20	181	198	173	142	48	37	47
21st	163	214	167	197	53	65	48
Jan.22	92	163	115	94	37	50	39
Jan.23	155	166	163	126	70	82	65
Jan.24	111	140	107	91	40	50	44
Jan.25	133	206	143	124	69	83	69

APPENDIX I, Table 6 (2)

DATE	S	A_o	B_o	C_o	S	A_p	B_p
Jan.26	112	240	149	142	58	89	60
Jan.27	138	209	152	168	65	84	66
Jan.28	193	281	205	170	74	80	72
Jan.29	115	208	116	97	42	80	68
Jan.30	125	240	144	127	37	67	41
Jan.31	130	200	155	122	66	80	61
Feb. 1	261	315	275	295	94	76	76
Feb. 2	246	363	247	223	130	126	119
Average:	148	205	157	144	59	74	62
RE:		-.39	-.06	.03		-.25	-.05

APPENDIX II

Figures *

* On surface maps the pressure values over 1000 mb the thousand digit is omitted

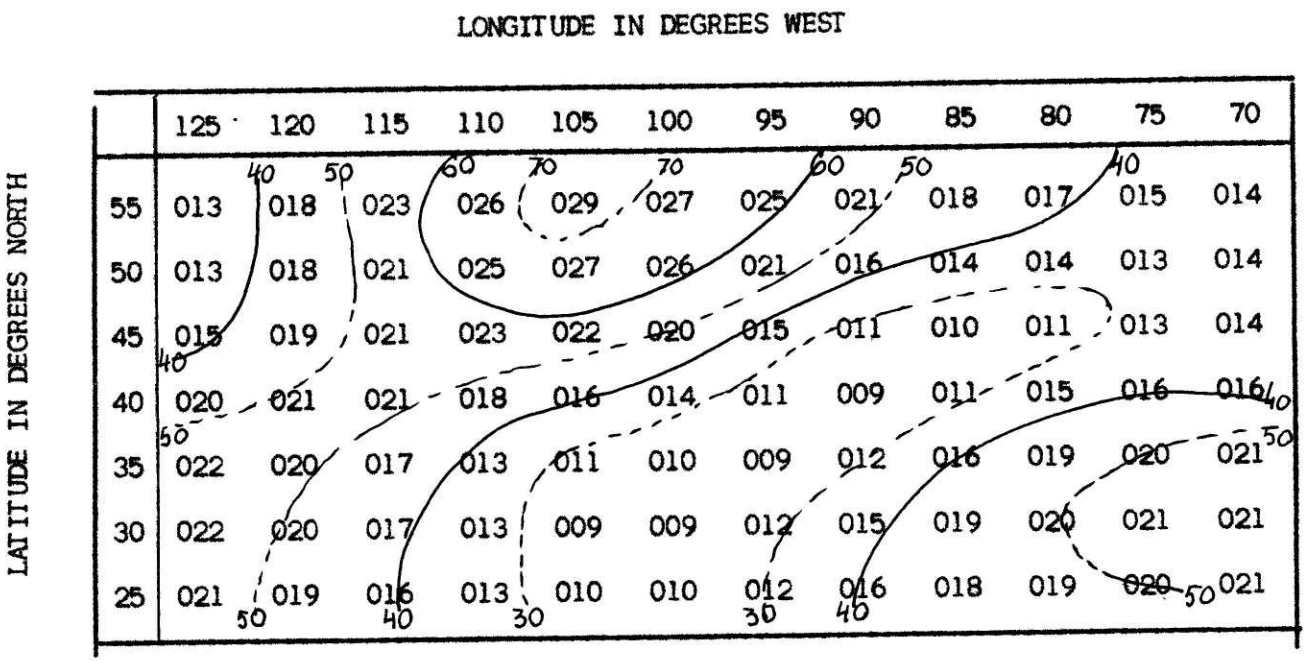

Fig. 2. January 4, 1230Z, Two-Map Prediction

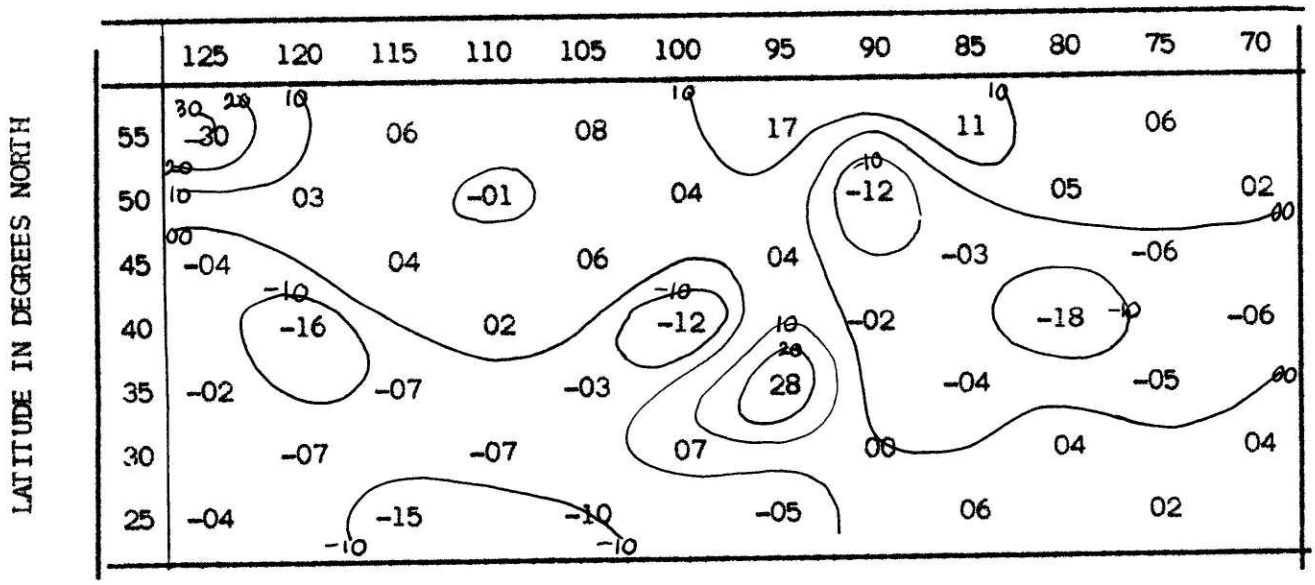

Fig. 3. January 3, 1530Z, 500-mb Vorticity Map

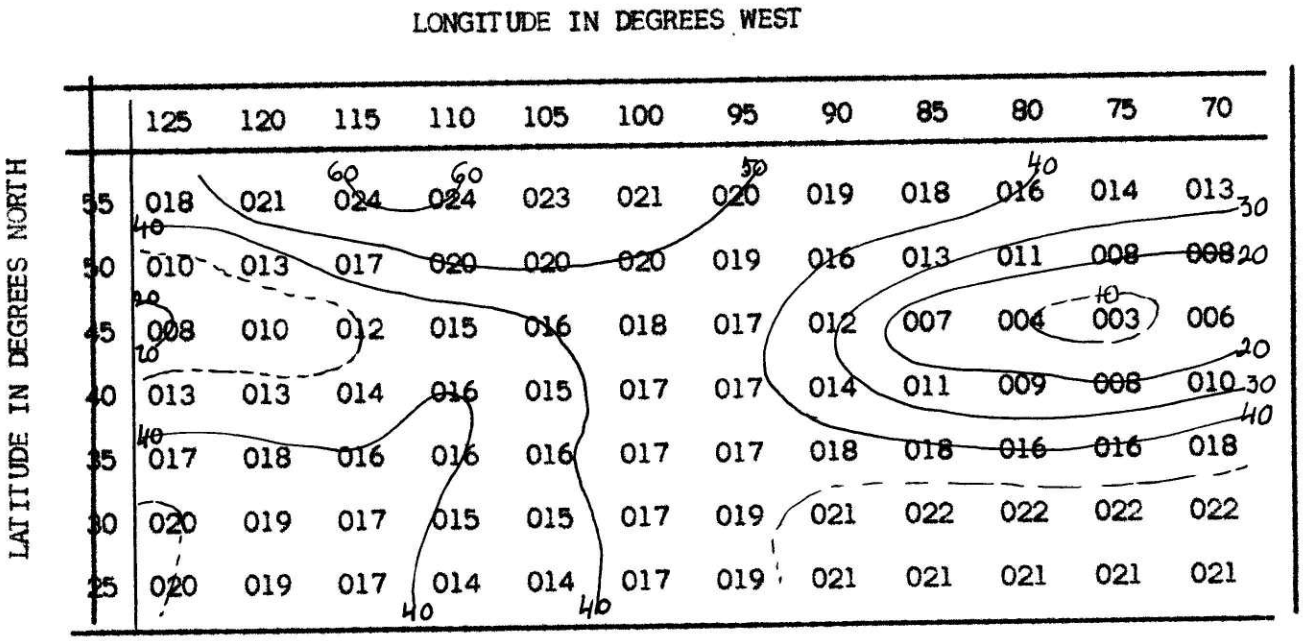

Fig. 4. January 4, 1230Z, Sea-Level Map

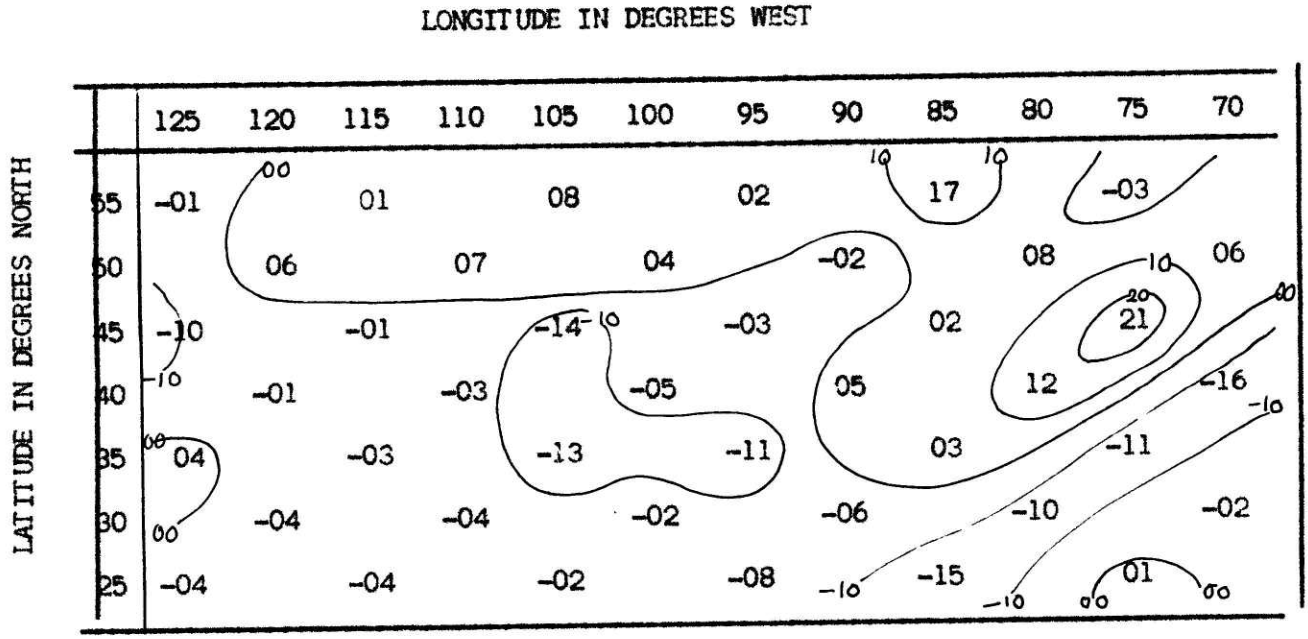

Fig. 5. January 4, 1530Z, Vorticity Map

LONGITUDE IN DEGREES WEST

LATITUDE IN DEGREES NORTH

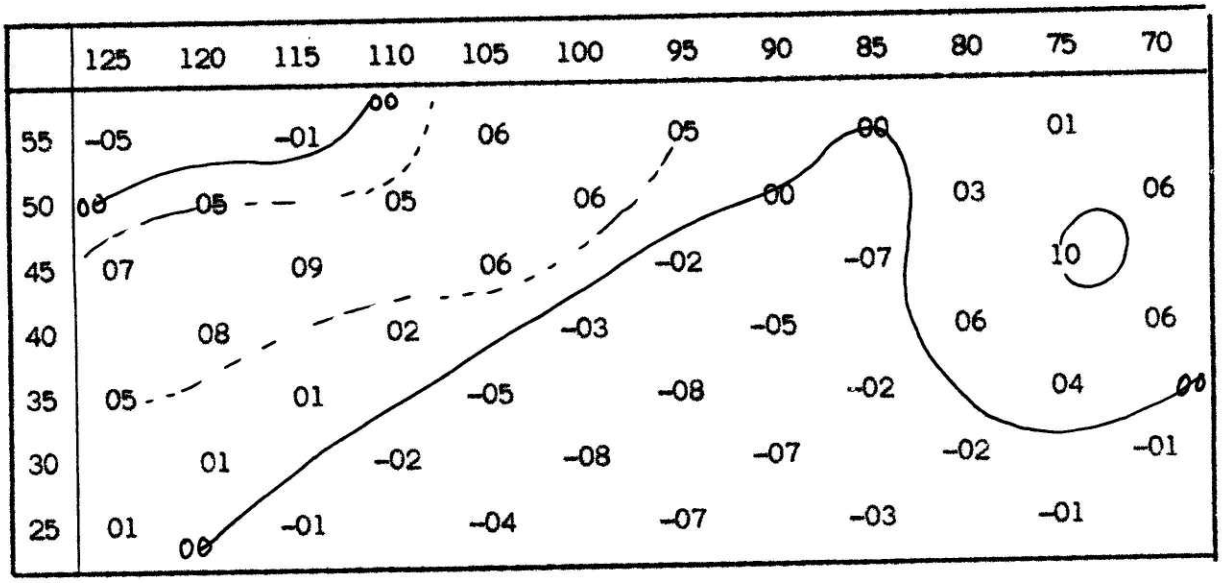

Fig. 6. January 4, 1230Z, Error Map

LONGITUDE IN DEGREES WEST

LATITUDE IN DEGREES NORTH

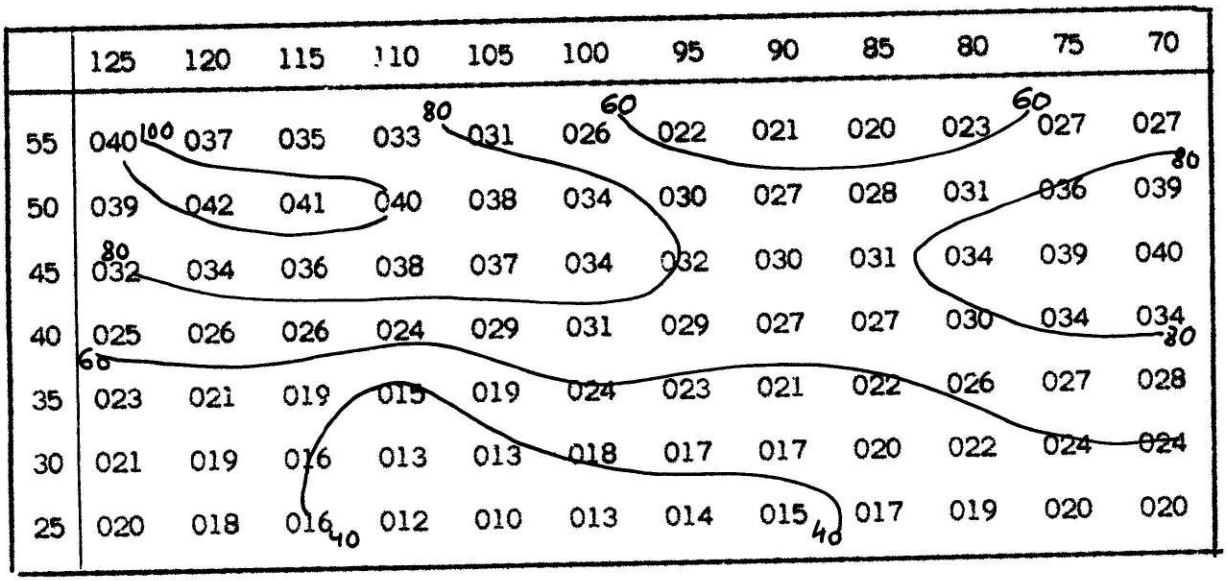

Fig. 7. January 31, 1230Z, Sea-Level Map

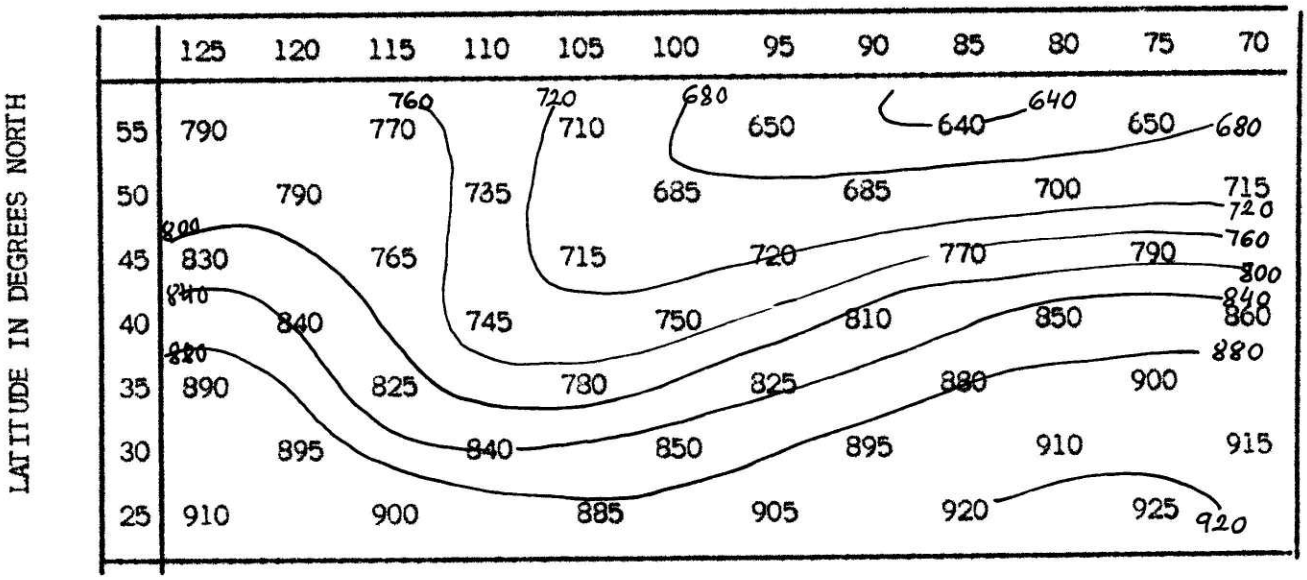

Fig. 8. January 31, 1530Z, 500-mb Map

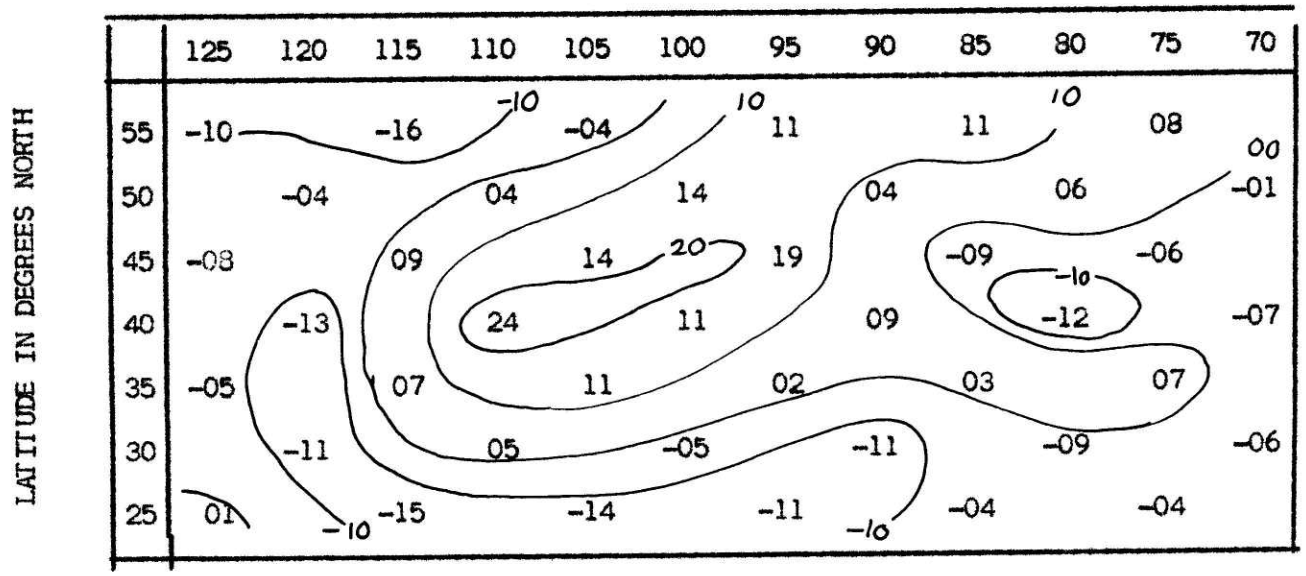

Fig. 9. January 31, 1530, Vorticity Map

LONGITUDE IN DEGREES WEST

LATITUDE IN DEGREES NORTH

	125	120	115	110	105	100	95	90	85	80	75	70
55	016	018	019	015	011	006	003	005	007	010	014	014
50	021	024	021	018	016	014	016	016	015	014	013	014
45	023	027	032	029	024	024	028	023	017	010	006	008
40	025	030	034	037	034	034	035	029	020	011	006	009
35	026	026	028	030	034	037	035	029	021	015	014	017
30	025	023	021	021	028	034	032	028	025	022	022	025
25	022	021	018	017	020	029	028	025	023	022	023	023

Fig. 10. February 1, 1230Z, Sea-Level Map

LONGITUDE IN DEGREES WEST

LATITUDE IN DEGREES NORTH

	125	120	115	110	105	100	95	90	85	80	75	70
55	-023	-019	-016	-018	-019	-020	-019	-015	-013	-013	-012	-012
50	-017	-018	-019	-021	-022	-019	-014	-011	-012	-016	-023	-025
45	-008	-006	-003	-008	-013	-010	-004	-006	-014	-024	-032	-031
40	-000	004	007	012	004	002	005	002	-006	-018	-027	-025
35	002	005	009	015	014	013	012	008	-000	-011	-013	-010
30	003	004	005	008	014	016	014	010	004	000	-002	000
25	002	003	002	004	009	015	014	010	005	002	002	002

Fig. 11. February 1, 1230Z,Sea-Level Pressure Change

LONGITUDE IN DEGREES WEST

LATITUDE IN DEGREES NORTH

	125	120	115	110	105	100	95	90	85	80	75	70
55	016	015	014	011	008	008	007	008	007	005	005	005
50	018	017	014	011	010	012	016	016	014	011	009	008
45	020	021	022	019	015	018	024	024	019	013	010	009
40	021	023	026	029	026	026	030	028	022	014	010	009
35	022	022	023	025	028	030	030	025	018	013	011	012
30	022	020	019	018	024	029	026	022	018	016	015	017
25	020	020	017	015	017	024	023	020	018	017	017	018

Fig. 12. February 1, 1230Z, Two-Map Prediction

LONGITUDE IN DEGREES WEST

LATITUDE IN DEGREES NORTH

	125	120	115	110	105	100	95	90	85	80	75	70
55	14		06		12		16		07		01	
50		08		10		14		06		03		07
45	03		-01		07		04		04		14	
40		-05		-08		00		-01		+07		11
35	-04		-06		-07		-06		-03		04	
30		-04		-05		-08		-08		-04		-04
25	02		-02		-06		-09		-06		-04	

Fig. 13. February 1, 1230Z, Error Map

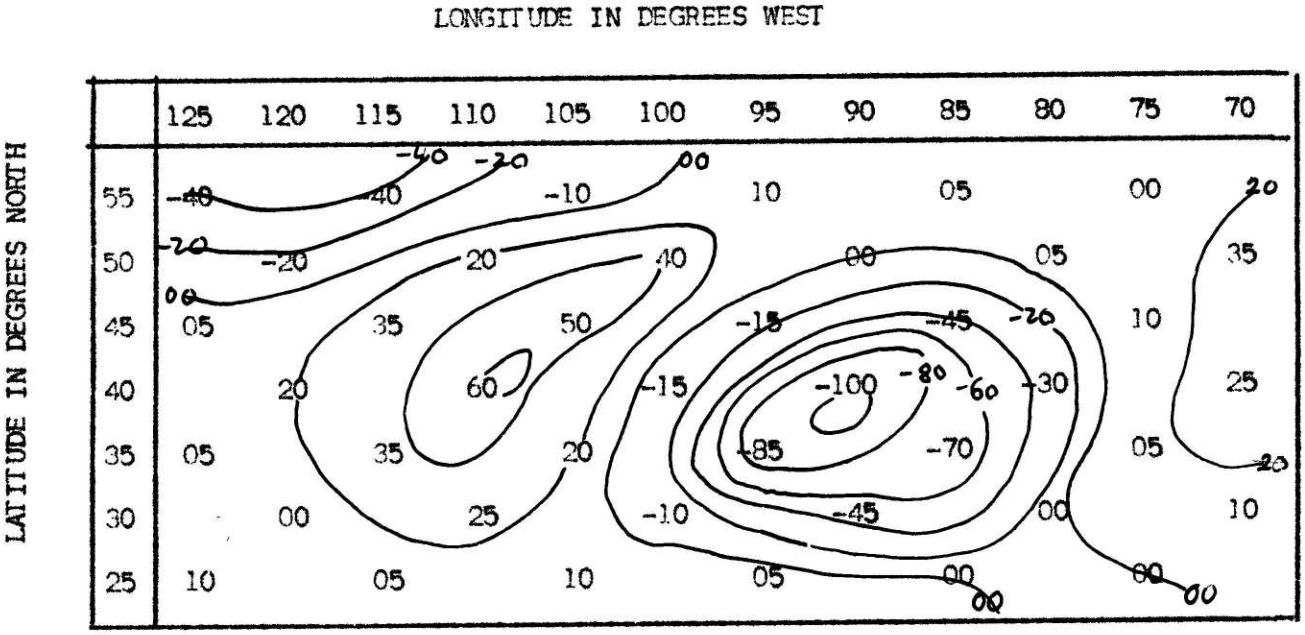

Fig. 14. February 1, 1530Z, 500-mb Change

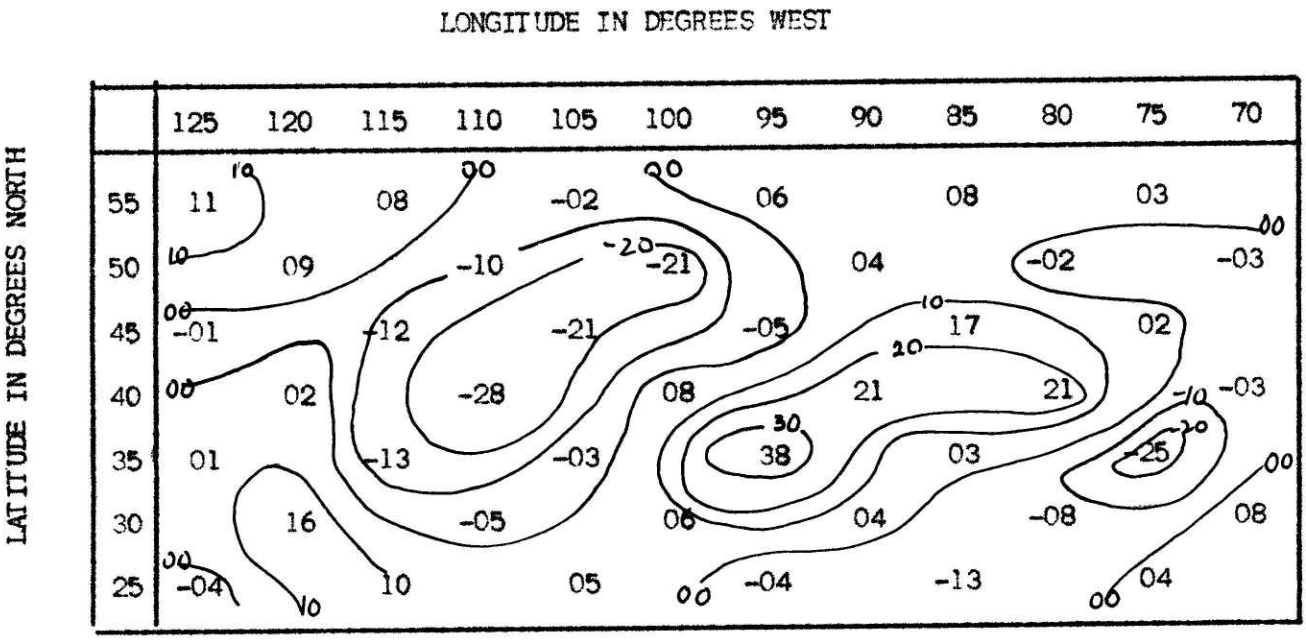

Fig. 15, February 1, 1530Z, Vorticity Change

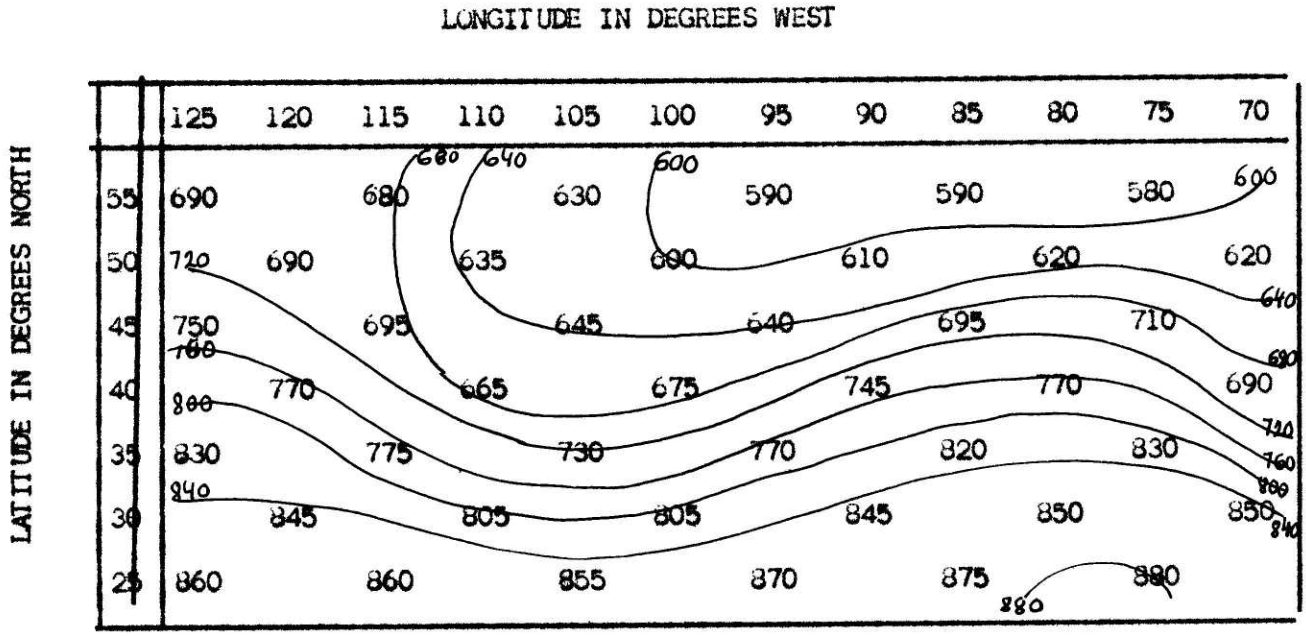

Fig. 16. January 31, 1530Z, 500/1000 Thickness Map

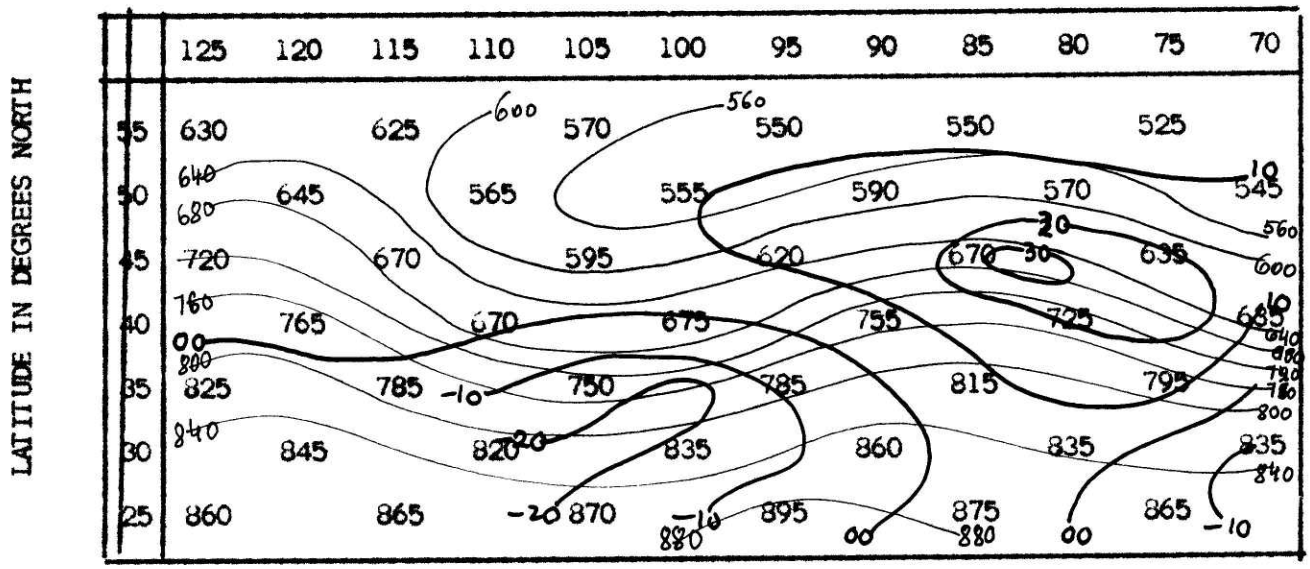

Fig. 17. February 1, 1530Z, 500/1000 Predicted Thickness Map and Predicted Thickness - Vorticity Map (Heavy Lines)

LONGITUDE IN DEGREES WEST

LATITUDE IN DEGREES NORTH

	125	120	115	110	105	100	95	90	85	80	75	70
55	014	017	018	015	012	006	002	998	995	992	991	992
50	014	015	015	013	009	006	003	001	000	999	997	995
45	017	021	022	018	012	009	010	010	010	008	007	003
40	022	025	028	031	021	017	019	023	025	022	016	011
35	023	024	026	028	026	024	028	031	030	025	021	017
30	023	022	021	021	025	029	031	031	029	026	022	020
25	022	021	019	017	021	029	029	027	026	023	022	021

Fig. 18. February 2, 1230Z, Two-Map Prediction

LONGITUDE IN DEGREES WEST

LATITUDE IN DEGREES NORTH

	125	120	115	110	105	100	95	90	85	80	75	70
55	09		05		-01		-05		-08		-11	
50		07		01		-08		-10		-10		-11
45	10		-01		-06		-12		-10		-07	-10
40		-02		-11		-12		-11		-05		-01
35	-02		-07		-12		-10		-04		00	
30		-04		-05		-09		-05		-01		00
25	-02		-02		-03		-05		-01		00	

Fig. 19. February 2, 1230Z, Error Map

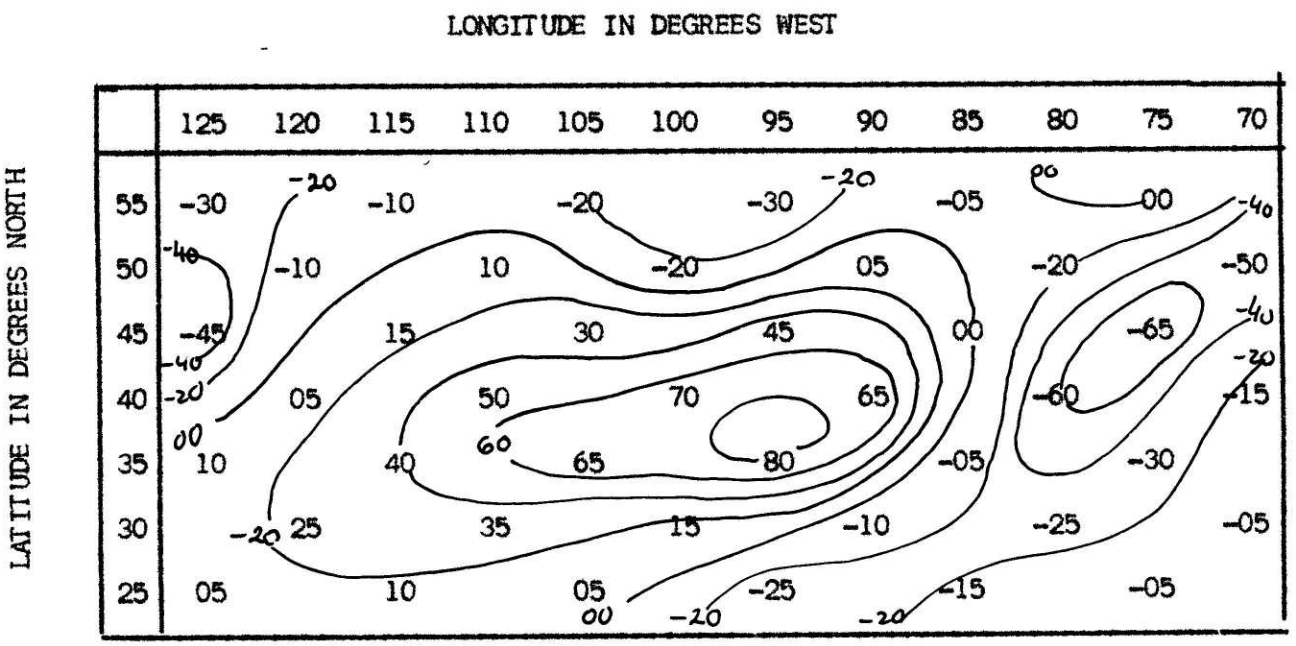

Fig. 20. February 2, 1530, 500-mb Height Change

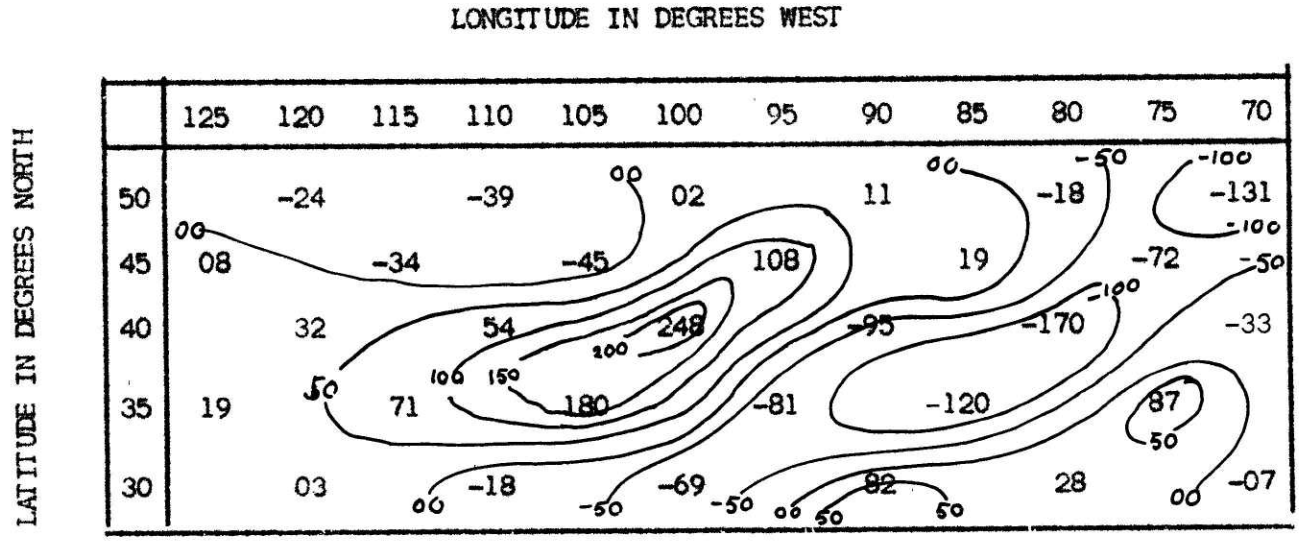

Fig. 21. February 2, 1530Z, "Jacobian Map"

APPENDIX II - Grid Points by Different Methods

	125	120	115	110	105	100	95	90	85	80	75	70 °W
55°N	o	.	o	.	o	.	o	.	o	.	o	.
50	.	o	.	o	.	x	.	x	.	x	.	x
45	o	.	o	.	o	.	x	.	x	.	x	.
40	.	o	.	o	.	x	.	x	.	x	.	x
35	o	.	o	.	o	.	x	.	x	.	x	.
30	.	o	.	o	.	x	.	x	.	x	.	x
25	o	.	o	.	o	.	o	.	o	.	o	.

Fig. 22. . 84 pressure points (statistical method)
o 42 vorticity and height points (A, B, C methods)
x 18 points for trajectory method

	135	130	125	120	115	110	105	100	95	90	85	80	75	70	65	60 °W
60°N				x		x		x		x		x		x		
55			x	.	x	.	x	.	x	.	x	.	x	.	x	
50		x	.	o	.	o	.	o	.	o	.	o	.	o	.	x
45	x	.	o	.	o	.	o	.	o	.	o	.	o	.	x	
40		x	.	o	.	o	.	o	.	o	.	o	.	o	.	x
35	x	.	o	.	o	.	o	.	o	.	o	.	o	.	x	
30		x	.	o	.	o	.	o	.	o	.	o	.	o	.	x
25			x	.	x	.	x	.	x	.	x	.	x	.	x	
20				x		x		x		x		x		x		

Fig. 23. o 30 points used in "Jacobian method"
. 47 vorticity points
x 36 additional values of height data